

Achieving 280fs resolution with a streak camera by reducing the deflection dispersion

Mahendra Man Shakya and Zenghu Chang

Citation: *Appl. Phys. Lett.* **87**, 041103 (2005); doi: 10.1063/1.2001732

View online: <http://dx.doi.org/10.1063/1.2001732>

View Table of Contents: <http://apl.aip.org/resource/1/APPLAB/v87/i4>

Published by the [American Institute of Physics](#).

Additional information on *Appl. Phys. Lett.*

Journal Homepage: <http://apl.aip.org/>

Journal Information: http://apl.aip.org/about/about_the_journal

Top downloads: http://apl.aip.org/features/most_downloaded

Information for Authors: <http://apl.aip.org/authors>

ADVERTISEMENT

**AIP**Advances

Submit Now

**Explore AIP's new
open-access journal**

- **Article-level metrics
now available**
- **Join the conversation!
Rate & comment on articles**

Achieving 280 fs resolution with a streak camera by reducing the deflection dispersion

Mahendra Man Shakya^{a)} and Zenghu Chang^{b)}

J.R. MacDonald Laboratory, Department of Physics, Kansas State University, Manhattan, Kansas 66506

(Received 1 February 2005; accepted 13 June 2005; published online 18 July 2005)

The factors that limit the temporal resolution in a streak camera operating in an accumulative mode were studied. By controlling the timing jitter, the transit-time dispersion and the technical resolution of the camera on the order of 100 fs, the role of the deflection dispersion was investigated experimentally. It was done by changing the electron beam size in the deflection plates with a variable slit in front of the plates. The temporal resolution of the camera reached 280 fs when the slit width was a 5 μm slit. © 2005 American Institute of Physics. [DOI: 10.1063/1.2001732]

X-ray streak cameras with resolutions of a few picoseconds have been used at the third generation synchrotrons to study ultrafast dynamics in solids and in plasmas.^{1–4} Because of the limited number of photons arriving on the streak camera and the low quantum efficiency of the photocathode, it is necessary to operate the streak camera in an accumulation mode.⁵ By reducing the timing jitter that used to be the factor dominating the accumulating camera, cameras with ~ 600 fs resolution have been developed in recent years.^{6,7} To study optical phonons with time resolved x-ray diffraction, it is desirable to use detectors with 100 fs resolution.⁸ In this letter, we focus on the reduction of the deflection dispersion in order to develop such a camera.

A schematic diagram of the streak tube used in this work is shown in the Fig. 1. The photocathode is a thin film of Au coated on a fused silica substrate. There is a 25 μm wide and 3 mm long slit on the anode to define the field of view of the camera. The single electrostatic quadrupole lens focuses the electron in the sweeping direction. A second slit is placed before the lens to control the electron transverse size in the lens and in the deflection plates, which is called the aperture stop slit. The meander type deflection plates have a response time of 120 ps. The electrons are intensified by a microchannel plate (MCP) and are displayed on a phosphor screen. The final streak image is recorded on charge-coupled-device (CCD) video camera. Using the video rate camera (Cohu 4920) instead of the slow-scan CCD allows real time optimization of the camera operation. The camera is cooled to 5 °C that allows signal accumulation up to 1 min.

The experimental setup for testing the camera is similar to that in Liu *et al.*⁷ To calibrate the scanning speed, a Mach-Zehnder interferometer was used to split the Kansas Light Source laser beam into two beams. Each beam contains two pulses with a predetermined time delay per laser shot. One beam is frequency converted into UV light by focusing the near infrared laser pulses in air. The laser pulse duration is 30 fs and the center wavelength is ~ 790 nm. The central wavelength of UV light is ~ 260 nm that is the third harmonics of the laser. The pulse duration of the UV pulse is expected to be less than 100 fs. The UV pulses produce photoelectrons from the photocathode. The other beam from the interferometer is incident on a GaAs photoconductive

switch. The near infrared laser pulses triggers the switch to generate ramp-voltage pulses for driving the deflection plates.⁷

The temporal resolution of an accumulative camera is limited by the timing jitter, the technical resolution, the transit time dispersion, and the deflection dispersion. In order to study the effects of the deflection dispersion, we tried to minimize the other factors that limit the temporal resolution. Timing jitter was the dominating factor for accumulative camera. It is caused by a fluctuation in the laser pulse energy absorbed by the photoconductive switch. In the last few years, the timing jitter has been significantly reduced as demonstrated by the work in Refs. 6 and 7. The photoconductive switch and the deflection plates of this camera is the same as that used in Ref. 7. The timing jitter is expected to be < 100 fs for the $\sim 1\% - 2\%$ rms energy fluctuation of the kilohertz laser used in the test.

The transit-time dispersion is the result of the initial energy spread of the liberated photoelectron from the surface of the photocathode. When the cathode is illuminated by x rays, the dispersion in the photocathode to anode region can be estimated by⁹ $\Delta t_{pa} = 2.63 \sqrt{\delta\epsilon/E}$, where $\delta\epsilon$ is in eV (the FWHM of electron energy distribution), electric field E is in kV/mm, and Δt_{pa} gives a time dispersion in ps. The initial energy distribution of Au under the 260 nm illumination is hard to find in literatures. The work function of polycrystalline Au is 5.1 eV,¹⁰ which is larger than the photon energy of the UV light used in the testing (4.7 eV). However, the contamination of the photocathode surface reduces the work function to 4.2–4.3 eV, which yields $\delta\epsilon = 0.5$ eV.¹⁰ The spread is smaller than with x rays, e.g., $\delta\epsilon = 1.1$ eV for KBr

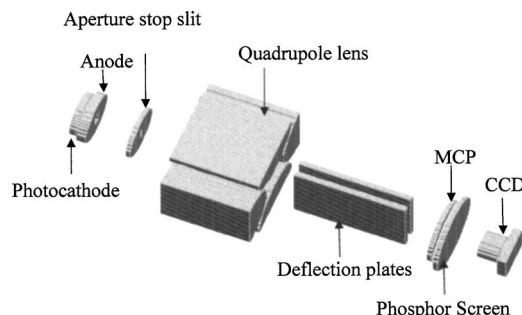


FIG. 1. Schematic of the streak tube with a slit that serves as the aperture stop.

^{a)}Electronic mail: mahendra@phys.ksu.edu

^{b)}Electronic mail: chang@phys.ksu.edu

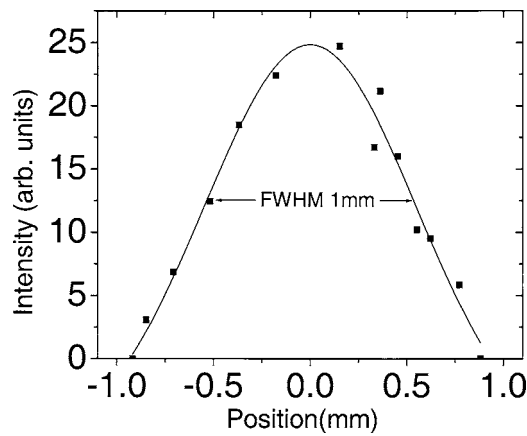


FIG. 2. The transverse profile of the electron beam at the aperture stop slit. The measured data are indicated by the squares. The solid line is from a curve fitting.

x-ray photocathode.¹¹ Thus, the test using UV light underestimates the transit temporal dispersion for application in x-ray detection applications. However, the interest of this paper is to study the effects of deflection aberrations. It is easier to observe the effects of deflection aberrations when the limitation to the resolution from other factors mentioned previously are minimized.

It is well known that increasing the electric field between the photocathode and the anode reduces the effect of photoelectron energy spread thereby improving the temporal resolution of the streak camera. A significant obstacle to implementing high field is the arcing that occurs between the cathode and the anode. We prevented the arcing by improving the vacuum and by polishing the photocathode and the anode. The highest electric field that our camera can sustain is 13.75 kV/mm while operated at the pressure 2×10^{-9} Torr, which gives $\Delta t_{pa} = 136$ fs.

The entrance slit limited resolution (technical resolution) of the camera is determined by $\Delta t_{tech} = \Delta X/V$, where V is the scanning speed, and ΔX is the static image width. The scanning speed of the camera is $0.84 \mu\text{m}/\text{fs}$, i.e., 2.8 times the velocity of the light. Such a fast speed was obtained with meander-type deflection plates driven by a GaAs switch. Because of the high deflection sensitivity ($0.67 \text{ mm}/\text{V}$) and fast response (120 ps), the ramp voltages applied on the deflection plates is low ($\pm 187 \text{ V}$).

To reduce the width of the slit image, we used electrostatic quadruple lens because of its smaller spherical aberration as compared to lenses with axial symmetry.¹² The measured image width ΔX was $166 \mu\text{m}$ when the entrance aperture slit was removed, which is much larger than ideal image width $52.1 \mu\text{m}$ obtained by multiplying anode slit width ($25 \mu\text{m}$) and the transverse magnification ($\times 2.1$). Evidently, this image broadening was caused by the aberrations inherent in the focusing lens and the MCP intensifier. The aberrations of the lens were reduced by placing a $5 \mu\text{m}$ slit in front of the lens. The static image width obtained with the $5 \mu\text{m}$ slit is $77 \mu\text{m}$, which is close to the ideal value and is the limit of the spatial resolution of the MCP intensifier. The measured transverse profile of the electron beam is shown in Fig. 2, which was measured by scanning a $25 \mu\text{m}$ slit across the electron beam at the entrance of the quadruple lens. The FWHM of the beam is $\sim 1 \text{ mm}$, thus, the aperture stop slit significantly reduced the size of the electron in the lens. The

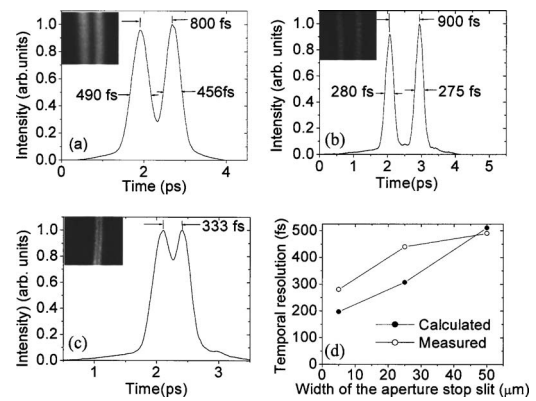


FIG. 3. The measured and calculated temporal resolution with various slits. (a) The slit width is $50 \mu\text{m}$. (b) The slit width is $25 \mu\text{m}$. (c) The slit width is $5 \mu\text{m}$. (d) Comparison of measured temporal resolution with the calculations.

technical resolution, Δt_{tech} with the $5 \mu\text{m}$ aperture stop slit is estimated to be 92 fs.

The ability of controlling the timing jitter, the transient-time dispersion and technical resolution on the other of 100 fs allowed us to study the deflection aberrations effectively. The deflection aberrations are caused by the finite electron transverse size and the transverse variation of the electric potential. The electrons travel faster in the higher potential region than those in the lower potential region. The difference of transit time in the plates can be estimated by¹³ $\Delta t_d = d\alpha/v_a$, where d is the transverse size of the electron beam in the deflection plates. The maximum deflection angle α and the average axial velocity v_a are 0.015 rad and $1.6 \times 10^{-3} \mu\text{m}/\text{fs}$, respectively, for our camera.

We studied the effects of the electron beam size in the deflection plates on the temporal resolution. The size was changed by using aperture stop slits with different widths. The results obtained are shown in the Figs. 3(a)–3(c). Figures 3(a) and 3(b) were obtained when slits of widths were $50 \mu\text{m}$ and $5 \mu\text{m}$. The corresponding results are summarized in Fig. 3(d). The two pulses with known delay were produced with a Mach-Zehnder interferometer. The results of these measurements clearly indicate that the resolution of the camera improves with the decrease in the beam size in the deflection plates. The temporal resolution of 280 fs by the conventional FWHM definition was obtained by using a $5 \mu\text{m}$ slit, as shown in Fig. 3(b). With such a camera, two pulses separated by 333 fs can be well resolved, as shown in Fig. 3(c).

The sizes of the electron beam at the entrance of the deflection plates was not measured. The sizes are expected to be close to the widths of the slits. The calculated dispersions caused by the deflection are 50 fs and 500 fs for a $5 \mu\text{m}$ slit width and a $50 \mu\text{m}$ width slit, respectively. The calculated result with a $50 \mu\text{m}$ width slit is close to the measured value. However, the estimated dispersion due to a beam size of $5 \mu\text{m}$ is much better than the measured value. This is not surprising since for such a resolution other limiting factors take over. The resolution Δt that includes all the previously mentioned effects can be estimated by $\Delta t = \sqrt{\Delta t_{jitter}^2 + \Delta t_{pa}^2 + \Delta t_{tech}^2 + \Delta t_d^2}$. The estimated values are indicated in Fig. 3(d). The calculated resolutions agree with the measured results.

Just like there is a compromise between the spatial resolution and the $f^\#$ of a conventional optical imaging system, a

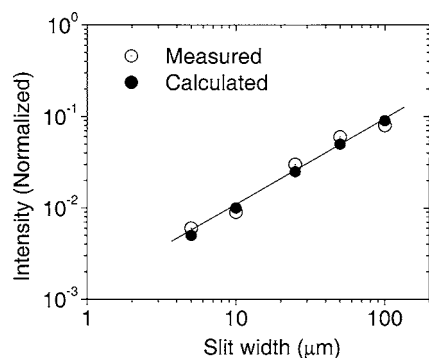


FIG. 4. Measured and estimated signal intensities as a function of the width of the aperture stop slit. The intensity is normalized to that when the slit is removed. The line is for guiding the eyes only.

compromise between the temporal resolution and the throughput of the streak tube must be made. The calculated relative signal intensities for various slit widths are shown in Fig. 4. The calculation was based on the transverse profile of the electron beam shown in Fig. 2 and the slit widths. As a comparison, the signal intensities were measured directly by changing the slit width, as shown in Fig. 4. The calculations are in agreement with the measurements. For an accumulative streak camera, a long integration time can compensate the reduction of the throughput.

In summary, we have shown experimentally that the deflection dispersions are a major limiting factor for streak cameras with resolutions approaching 100 fs. It is clear that the deflection aberrations can be reduced by reducing the beam size of the electron in the deflection plates. We demonstrated that a resolution of 280 fs FWHM was achieved when with a 5 μm wide slit was used. X-ray streak cameras with such a high resolution can not only enhance the research capabilities at the third generation synchrotron facility, but will also impact the development and applications of

the fourth generation x-ray sources. The camera may also become an important diagnostics for the development of the fourth generation x-ray sources whose pulse duration is on the order of 100 fs.

This work is supported by the Division of Chemical Science, Office of Basic Energy Science, and the U.S. Department of Energy. We would like to thank J. Liu for his invaluable help. The supports from B. Shan, C. Wang, and J. Xia at the Kansas Light Source Facility are greatly appreciated.

- ¹A. M. Lindenberg, I. Kang, S. L. Johnson, T. Missalla, P. A. Heimann, Z. Chang, J. Larsson, P. H. Bucksbaum, H. C. Kapteyn, H. A. Padmore, R. W. Lee, J. S. Wark, and R. W. Falcone, *Phys. Rev. Lett.* **84**, 111 (2000).
- ²A. M. Lindenberg, I. Kang, S. L. Johnson, R. W. Falcone, P. A. Heimann, Z. Chang, R. W. Lee, and J. S. Wark, *Opt. Lett.* **27**, 869 (2002).
- ³M. F. DeCamp, D. A. Reis, A. Cavalieri, P. H. Bucksbaum, R. Clarke, R. Merlin, E. M. Dufresne, D. A. Arms, A. Lindenberg, A. Macphee, Z. Chang, J. S. Wark, and B. Lings, *Phys. Rev. Lett.* **91**, 165502 (2003).
- ⁴S. L. Johnson, P. A. Heimann, A. M. Lindenberg, H. O. Jeschke, M. E. Garcia, Z. Chang, R. W. Lee, J. J. Rehr, and R. W. Falcone, *Phys. Rev. Lett.* **91**, 157403 (2003).
- ⁵J. Larsson, Z. Chang, E. Judd, P. J. Schuck, R. W. Falcone, P. A. Heimann, H. A. Padmore, H. C. Kapteyn, P. H. Bucksbaum, M. M. Murnane, R. W. Lee, A. Machacek, J. S. Wark, X. Liu, and B. Shan, *Opt. Lett.* **22**, 1012 (1997).
- ⁶G. A. Naylor, K. Scheidt, J. Larsson, M. Wulff, and J. M. Filholl, *Meas. Sci. Technol.* **12**, 1858 (2001).
- ⁷Jinyuan Liu, Jin Wang, Bing Shan, Chun Wang, and Zenghu Chang, *Appl. Phys. Lett.* **82**, 3553 (2003).
- ⁸A. Rousse, C. Rischel, and J.-C. Gauthier, *Rev. Mod. Phys.* **73**, 17 (2001).
- ⁹Z. Chang, A. Rundquist, J. Zhou, M. M. Murnane, H. C. Kapteyn, X. Liu, B. Shan, J. Liu, L. Niu, M. Gong, and X. Zhang, *Appl. Phys. Lett.* **69**, 133 (1996).
- ¹⁰Xinrong Jiang, C. N. Berglund, and Anthony E. Bell, and William A. Mackie, *J. Vac. Sci. Technol. B* **16**, 3374 (1998).
- ¹¹B. L. Henke, J. Liesegang, and S. D. Smith, *Phys. Rev. B* **19**, 3004 (1979).
- ¹²S. Okayama and H. Kawakatsu, *J. Phys. E* **16**, 166 (1983).
- ¹³P. A. Jaanimagi, *Proc. SPIE* **5194**, 171 (2004).